ACS Medicinal Chemistry Letters

Letter

pubs.acs.org/acsmedchemlett

Discovery and Development of Potent and Selective Inhibitors of Histone Methyltransferase G9a

Ramzi F. Sweis,*[,†] Marina Pliushchev,[†] Peter J. Brown,[‡] Jun Guo,[†] Fengling Li,[‡] David Maag,[†] Andrew M. Petros,[†] Nirupama B. Soni,[†] Chris Tse,[†] Masoud Vedadi,[‡] Michael R. Michaelides,[†] Gary G. Chiang,[†] and William N. Pappano[†]

[†]Discovery Research, AbbVie Inc., 1 North Waukegan Road, North Chicago, Illinois 60064, United States

[‡]Structural Genomics Consortium, University of Toronto, Toronto, Canada

Supporting Information

ABSTRACT: G9a is a histone lysine methyltransferase responsible for the methylation of histone H3 lysine 9. The discovery of A-366 arose from a unique diversity screening hit, which was optimized by incorporation of a propyl-pyrrolidine subunit to occupy the enzyme lysine channel. A-366 is a potent inhibitor of G9a (IC_{50}: 3.3 nM) with greater than 1000-fold selectivity over 21 other methyltransferases.

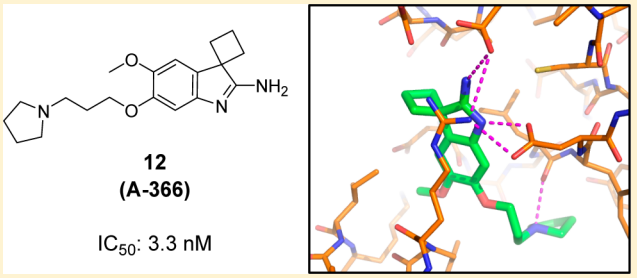

KEYWORDS: *G9a, methyltransferase, A-366, methylation, epigenetics*

Histone methyltransferases (HMTs), a class of enzymatic "writers" of epigenetic marks, have recently emerged as targets of potential therapeutic value.[1,2] They catalyze the methylation of histone lysines and arginines utilizing S-adenosyl-methionine (SAM) as the cofactor/methyl-source. This process can result in either the activation or repression of transcription.[3,4] Dysregulation of methylation at specific histone sites (alterations in the "histone code") has been implicated in many cancers.[5−7] Hence, targeting HMT activity has been the subject of much investigation in the field of oncology, even recently reaching human clinical trials.[8]

Euchromatic histone methyltransferase 2 (EHMT2), also known as G9a, is an HMT that is primarily responsible for the dimethylation of lysine 9 on histone H3 (H3K9). Several reports have highlighted its link to a variety of cancers. It is upregulated in hepatocellular carcinoma,[9] B cell acute lymphoblastic leukemia,[10] and lung cancers.[11] In addition, elevated expression of G9a in aggressive lung cancer correlates with poor prognosis, while its knockdown in highly invasive lung cancer cells suppressed metastasis in an in vivo mouse model.[12] In prostate cancer cells (PC3), G9a knockdown caused significant morphological changes and inhibition of cell growth.[13]

While small molecule inhibitors of G9a (Figure 1) have been reported as early as 2005,[14] BIX01294 (**1**) was the first reported potent and selective inhibitor.[15] It was found to reduce H3K9 dimethyl levels in cells and notably was not a SAM-competitive inhibitor. Recently, a second G9a inhibitor, UNC0638 (**2**), was disclosed. Quinazoline **2**, which incorporated a lysine-mimic via an *n*-propyl-pyrrolidine exhibited a >10-fold enhancement in potency over **1** along with selectivity over a panel of 17 other epigenetic targets.[16−19]

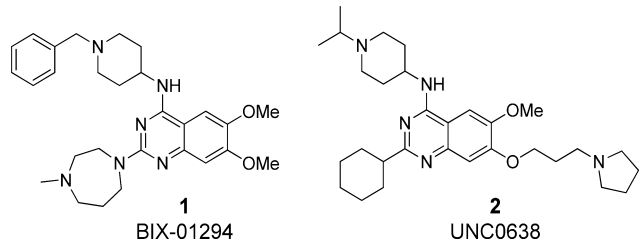

Figure 1. Selective small molecule inhibitors of G9a.

Our efforts toward the identification of chemically distinct G9a inhibitors commenced with a chemical diversity subset screen of our compound collection. The assay format employed was a peptide-based AlphaLISA, measuring the levels of H3K9 dimethylation. Several clusters of related chemical matter were identified, but a singleton stood out: spiro[cyclobutane-1,3′-indol]-2′-amine (**3**) as having robust potency (IC_{50}: 153 nM). The low molecular weight of this compound translated to a high binding efficiency index (BEI) value of 27.[20] Such a feature rendered **3** as an attractive starting point for chemistry efforts aimed at further potency optimization.

The importance of the various subunits of **3** was initially interrogated by evaluation of a few closely related analogues (Table 1). Interestingly, the cyclobutyl group in **3** was an ideal

Received: December 3, 2013
Accepted: January 2, 2014
Published: January 2, 2014

Table 1. Potency of Amino-Indole Screening Hit 3 and Closely Related Analogues

Compound	Amino-indole	AlphaLISA IC50 (μM)
3	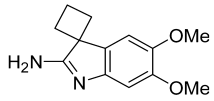	0.153
4	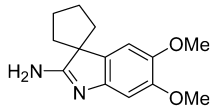	2.46
5	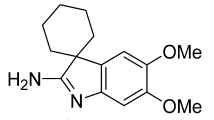	3.54
6	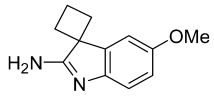	18.2
7	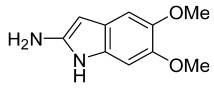	14.4

ring size, as cyclopentyl (**4**) and cyclohexyl (**5**) analogues were much less potent (IC_{50}: 2.46 and 3.54 μM, respectively (Table 1). In an example where one of the methoxy subunits was omitted (**6**), potency was reduced to 18.2 μM. Complete removal of the ring substitution at the 3-position of the indole, as in compound **7**, also resulted in a significantly attenuated IC_{50} value of 14.4 μM.

The spiro[cycloalkyl-1,3′-indol]-2′-amines were synthesized by the route shown in Scheme 1. Bis-alkylation at the benzylic

Scheme 1. Synthesis of 2-Amino-3-cycloakylindoles[a]

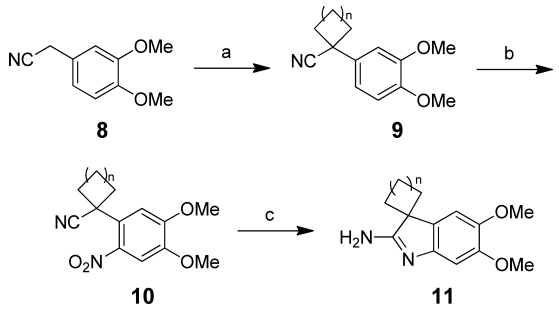

[a]Reagents and conditions: (a) NaH, THF, 0 °C dibromopropane (for n = 1); (b) HNO_3, $AcOH/Ac_2O$ 0 °C; (c) H_2, 10% Pd/C, 3 h.

carbon of **8** was achieved with sodium hydride and the corresponding dibromoalkane. Nitration of the phenyl ring followed by reduction of the nitro group led to compounds represented by **11**.

The presence of the *ortho*-dimethoxy-moiety in these compounds warranted comparison to the quinazoline core of **1** and **2**. As such, it was speculated that our inhibitor was also a peptide-competitive inhibitor. By utilizing this core to anchor a subunit that would occupy the lysine channel of G9a, it was hypothesized that further potency gains would be realized. As shown in Table 2, several lysine mimetics were evaluated as candidates for replacement of one of the *ortho*-methoxy groups.

Table 2. Evaluation of Amine-Containing Derivatives of Amino-indoles

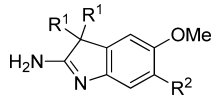

Compound	R^1	R^2	AlphaLISA IC_{50} (nM)
12 (A-366)		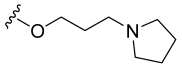	3.3
13		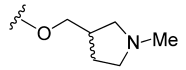	1.0
14		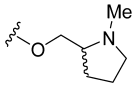	5.0
15		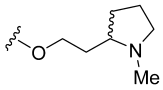	150
16		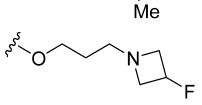	4.8
17		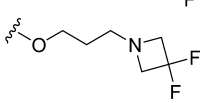	1342
18		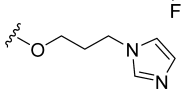	754
19		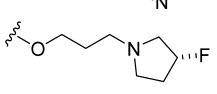	3.7
20		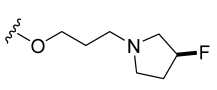	18
21		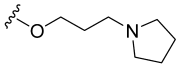	0.9
22		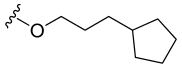	12900

Pyrrolidine **12** (A-366) exhibited a remarkable improvement in potency (IC_{50}: 3.6 nM) over **3** highlighting the beneficial impact of this approach. Variants of this were also evaluated, including the methyl pyrrolidines **13** and **14**, which were similar in potency (IC_{50}: 1.0 and 5.0 nM, respectively). A third analogue, **15**, contains a methyl pyrrolidine ring further extended from the core than in either **13** or **14**. This resulted in an attenuated potency (IC_{50}) of only 150 nM. Fluoro-azetidines were also evaluated in place of the pyrrolidine (entry **16** and **17**). The monofluoro analogue displayed similar potency to **12** (IC_{50}: 4.6 nM), whereas the difluoro analogue was 2 orders of magnitude less potent (IC_{50}: 1342 nM). This may be attributed to the reduced basicity of the azetidine nitrogen caused by the extra fluorine substitution.[21] Installing an imidazole (**18**, IC_{50}: 754 nM) reinforced the notion that a basic nitrogen would be critical for effective enzyme inhibition. Substitution of fluorine on the pyrrolidine ring of **12** was evaluated next, with *R*- and *S*-fluoro-pyrrolidines **19** and **20** exhibiting robust potency with a slight preference of one enantiomer (**19**, IC_{50}: 3.7 nM) over the other (**20**, IC_{50}: 18 nM).

dx.doi.org/10.1021/ml400496h | ACS Med. Chem. Lett. 2014, 5, 205−209

Finally, replacing the cyclobutyl subunit with a geminal dimethyl group (**21**, R^1 = Me) yielded a slight potency boost (IC_{50}: 0.9 nM). With this core, the importance of the pyrrolidine nitrogen was directly addressed by substituting with a cyclopentyl group (**22**), which diminished potency by 4 orders of magnitude (IC_{50}: 12,900 nM).

The synthesis of the compounds depicted in Table 2 followed the general strategy shown in Scheme 2. Commencing

Scheme 2. Synthetic Route to 12 and Related Analogues[b]

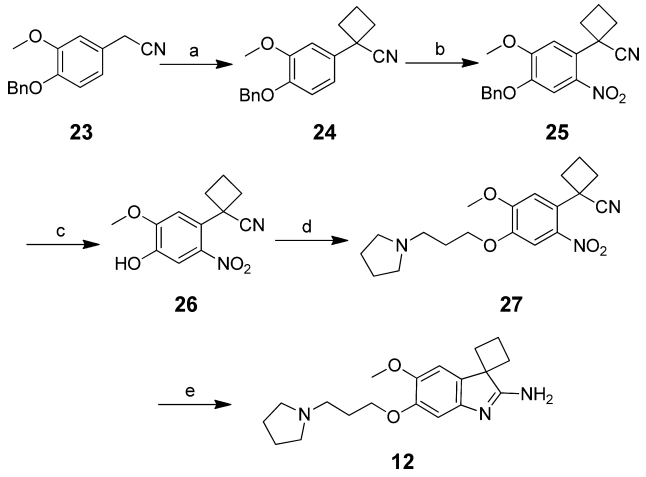

[b]Reagents and conditions: (a) NaOH, 1,3-dibromopropane, (n-Bu)$_4$NBr, toluene, 50%; (b) HNO_3, $AcOH/Ac_2O$, 0 °C, 92%; (c) 10% Pd/C, H_2, EtOH; (d) K_2CO_3, 1-(3-bromopropyl)pyrrolidine), 100 °C; (e) 10% Pd/C, H_2, AcOH, or Zn, AcOH.

with phenyl-acetonitrile **23**, dialkylation of the benzylic carbon with 1,3-dibromopropane proceeded under basic conditions. The resultant cyclobutyl derivative, **24**, was nitrated to provide **25**, from which the benzyl protective group was removed by hydrogenation to expose the phenol **26**. Subsequent alkylation with 1-(3-bromopropyl)pyrrolidine) proceeded at 100 °C with potassium carbonate. Cyclization to the final spiro[cycloalkyl-1,3′-indol]-2′-amine, **12**, was initiated by reduction of the nitro-group either under hydrogen gas and 10% palladium on carbon or with Zn in acetic acid.

To determine the mechanism of inhibition of G9a by **12**, the IC_{50} values were determined at various concentrations of SAM and peptide substrate (Figure 2). A linear increase of IC_{50} values as the peptide concentration was elevated indicates competitive inhibition with respect to peptide substrate. A decrease in IC_{50} values were observed as the SAM concentration was increased suggesting an uncompetitive inhibition with respect to SAM.

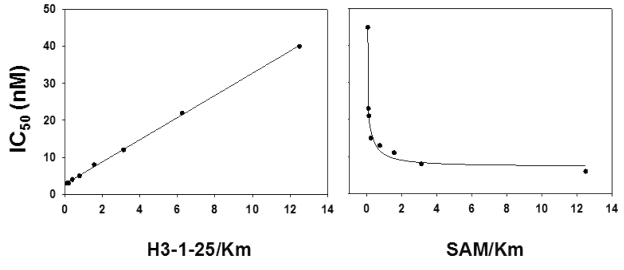

Figure 2. Mechanism of G9a inhibition by **12**: peptide-competitive vs SAM-uncompetitive.

The selectivity of **12** was also evaluated against 21 other methyltransferases using a scintillation proximity assay (SPA) format (Figure 3). Similar to the AlphaLISA result, the IC_{50} of

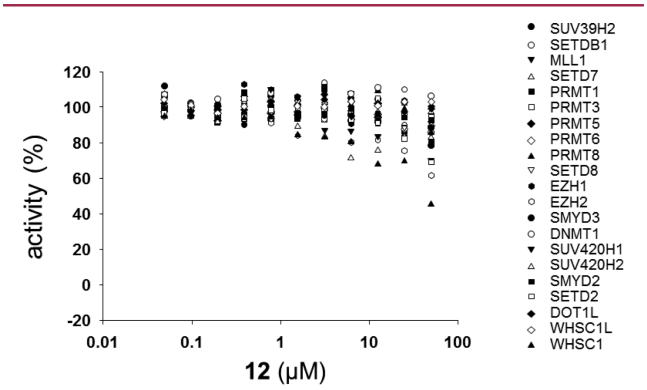

Figure 3. Selectivity of A-366 (**12**). Effect of **12** on the activity of 20 protein methyltransferases and DNMT1.

A-366 against G9a was 3 nM. No significant inhibition was observed for all other enzymes tested up to 50 μM (Figure 3). The only exception (not shown) was for GLP, (EHMT1, G9a-like protein), another HMT capable of dimethylation of H3K9. Compound **12** was only 10-fold less potent as a GLP inhibitor (IC_{50}: 38 nM). The modest selectivity is not surprising due to the high degree of homology (80% sequence identity) between the two.[22] It is similar, if not moderately improved, over the reported selectivity of other G9a inhibitors such as **2**.[17]

The potency and selectivity of **12** made it an ideal candidate to probe the function of G9a in cells. An In-Cell Western assay (H3K9Me2 antibody immunofluorescence) was performed after treating a human prostate cancer cell line, PC3, with compound **12** for 72 h (Figure 4). For comparison, the known

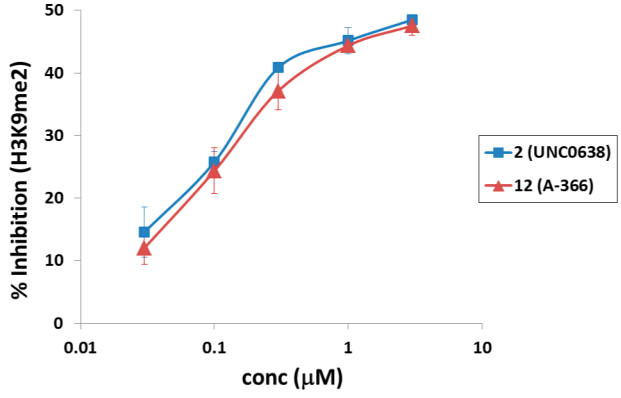

Figure 4. Inhibition of H3K9Me2 levels in PC3 cells after 72 h of treatment with G9a inhibitors.

G9a inhibitor **2** was evaluated in this study concurrently. The cellular levels of H3K9Me2 were noticeably reduced by nearly 50% at 3 μM for both compounds. In addition, the levels of total histone 3, H3K27Me3, and H3K36Me2 were unaltered in cells treated under similar conditions, confirming that the observed effect of these inhibitors was H3K9 specific.

To gain additional insight into the mode of binding of these compounds, we obtained a high-resolution X-ray cocrystal structure of **12** with G9a. The binding to the substrate peptide site on G9a involves a mix of both hydrophobic and electrostatic interactions (Figure 5). The side chain of L1086

dx.doi.org/10.1021/ml400496h | ACS Med. Chem. Lett. 2014, 5, 205−209

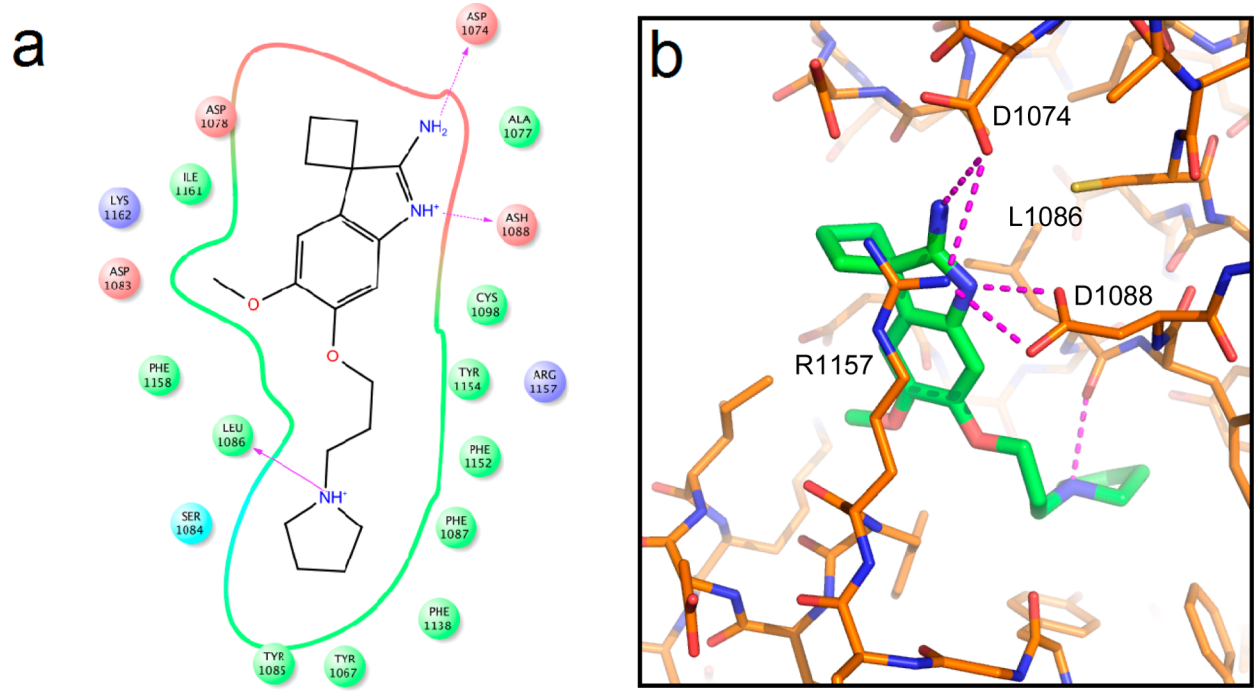

Figure 5. (a) Lysine channel of G9a highlighting the amino acid residues and their interactions with **12**. (b) X-ray cocrystal structure of **12** and G9a, revealing the orientation of key residues around the spiro[cycloalkyl-1,3′-indol]-2′-amine core and the pyrrolidine.

forms the hydrophobic wall of the pocket and is in van der Waals contact with the phenyl group of **12**. The methoxy moiety of the ligand sits in a hydrophobic dimple formed by the side chains of F1158, I1161, and the aliphatic portion of K1162.

The amidine nitrogen atoms of **12** form electrostatic hydrogen bonds with the side chain carboxylates of D1074 and D1088. In addition, the pyrrolidine nitrogen donates a hydrogen to the backbone carbonyl of L1086, while the carbon atoms of the pyrrolidine sit in a hydrophobic subpocket formed by the side chains of Y1067, F1087, F1152, Y1154, and F1158. This position of the pyrrolidine forces the two central methylene carbons of the four atom linker between the pyrrolidine and phenyl into a gauche conformation.

The side chain of R1157, well-ordered in the structure, packs against the face of the bound ligand opposite that of L1086 in a parallel fashion. The guanidine moiety of this arginine forms electrostatic hydrogen bonds to the side chain carboxylates of D1074 and D1088. The overall binding mode is similar to that previously observed for UNC0638.

In conclusion, through elaboration of a spiro[cycloalkyl-1,3′-indol]-2′-amine (**3**), we have identified chemically distinct, potent (low nM IC_{50}), and selective inhibitors of G9a. A-366 (**12**) was profiled extensively as an in vitro tool. A mechanism of action study has shown that **12** is a peptide-competitive inhibitor. In addition, it is highly selective over a panel of 21 other methyltransferases. Finally, it effects a clear reduction in H3K9 methylation in cells. These combined properties render it a valuable tool for precise interrogation of the role and function of G9a. In this regard, it is noteworthy that the core of **12** (a spiro[cycloalkyl-1,3′-indol]-2′-amine) represents a chemotype that is unrelated to the quinazoline core of **1** and **2**. Further characterization of the biological activity of A-366 and its biological differentiation from other known G9a inhibitors will be reported in due course.

■ ASSOCIATED CONTENT

Ⓢ Supporting Information

Experimental details are provided that pertain to the X-ray crystallography, biological assays, and the synthesis and characterization of compounds **1**−**27**. This material is available free of charge via the Internet at http://pubs.acs.org.

■ AUTHOR INFORMATION

Corresponding Author

*(R.F.S.) E-mail: ramzi.sweis@abbvie.com. Tel: 847-937-0315.

Funding

The design, study conduct, and financial support was provided by AbbVie & the SGC. AbbVie & the SGC participated in the data generation, interpretation of data, review, and approval of this publication. The SGC is a registered charity (number 1097737) that receives funds from AbbVie, Boehringer Ingelheim, Canada Foundation for Innovation, the Canadian Institutes for Health Research, Genome Canada through the Ontario Genomics Institute [OGI-055], GlaxoSmithKline, Janssen, Lilly Canada, the Novartis Research Foundation, the Ontario Ministry of Economic Development and Innovation, Pfizer, Takeda, and the Wellcome Trust [092809/Z/10/Z].

Notes

The authors declare the following competing financial interest: RFS, MP, JG, DM, AMP, NBS, CT, MRM, GGC, and WNP are employees of AbbVie Inc.

■ REFERENCES

(1) Portela, A.; Esteller, M. Epigenetic modifications and human disease. *Nat. Biotechnol.* **2010**, *28*, 1057−1068.

(2) Bissinger, E.-M.; Heinke, R.; Sippl, W.; Jung, M. Targeting epigenetic modifiers: Inhibitors of histone methyltransferases. *Med. Chem. Commun.* **2010**, *1*, 114−124.

(3) Martin, C.; Zhang, Y. The diverse functions of histone lysine methylation. *Nat. Rev. Mol. Cell Biol.* **2005**, *6*, 838−849.

(4) Jones, P. A.; Baylin, S. B. The epigenomics of cancer. *Cell* **2007**, *128*, 683−692.
(5) Chi, P.; Allis, C. D.; Wang, G. G. Covalent histone modifications: miswritten, misinterpreted and mis-erased in human cancers. *Nat. Rev. Cancer* **2010**, *10*, 457−469.
(6) Copeland, R. A.; Moyer, M. P.; Richon, V. M. Targeting genetic alterations in protein methyltransferases for personalized cancer therapeutics. *Oncogene* **2013**, *32*, 939−946.
(7) Schneider, R.; Bannister, A. J.; Kouzarides, T. Unsafe SETs: histone lysine methyltransferases and cancer. *Trends Biochem. Sci.* **2002**, *8*, 396−402.
(8) Sweis, R. F.; Michaelides, M. R. Recent advances in small-molecule modulation of epigenetic targets: discovery and development of histone methyltransferase and bromodomain inhibitors. *Annu. Rep. Med. Chem.* **2013**, *48*, 185−203.
(9) Kondo, Y.; Shen, L.; Suzuki, S.; Kurokawa, T.; Masuko, K.; Tanaka, Y.; Kato, H.; Mizuno, Y.; Yokoe, M.; Sugauchi, F.; Hirashima, N.; Orito, E.; Osada, H.; Ueda, R.; Guo, Y.; Chen, X.; Issa, J. P.; Sekido, Y. Alterations of DNA methylation and histone modifications contribute to gene silencing in hepatocellular carcinomas. *Hepatol. Res.* **2007**, *37*, 974−983.
(10) Huang, J.; Dorsey, J.; Chuikov, S.; Zhang, X.; Jenuwein, T.; Reinberg, D.; Berger, S. L. G9a and Glp methylate lysine 373 in the tumor suppressor p53. *J. Biol. Chem.* **2010**, *285*, 9636−9641.
(11) Watanabe, H.; Soejima, K.; Yasuda, H.; Kawada, I.; Nakachi, I.; Yoda, S.; Naoki, K.; Ishizaka, A. Deregulation of histone lysine methyltransferases contributes to oncogenic transformation of human bronchoepithelial cells. *Cancer Cell Int.* **2008**, *8*, 15.
(12) Chen, M.-W.; Hua, K.-T.; Kao, H.-J.; Chi, C.-C.; Wei, L.-H.; Johansson, G.; Shiah, S.-G.; Chen, P.-S.; Jeng, Y.-M.; Cheng, T.-Y.; Lai, T.-C.; Chang, J.-S.; Jan, Y.-H.; Chien, M.-H.; Yang, C.-J.; Huang, M.-S.; Hsiao, M.; Kuo, M.-L. H3K9 histone methyltransferase G9a promotes lung cancer invasion and metastasis by silencing the cell adhesion molecule Ep-CAM. *Cancer Res.* **2010**, *70*, 7830−7840.
(13) Kondo, Y.; Shen, L.; Ahmed, S.; Boumber, Y.; Sekido, Y.; Haddad, B. R.; Issa, J-P. J. Downregulation of histone H3 lysine 9 methyltransferase G9a induces centrosome disruption and chromosome instability in cancer cells. *PLoS One* **2008**, *3*, e2037.
(14) Greiner, D.; Bonaldi, T.; Eskeland, R.; Roemer, E.; Imhof, A. Identification of a specific inhibitor of the histone methyltransferase SU(VAR)3−9. *Nat. Chem. Biol.* **2005**, *1*, 143−145.
(15) Kubicek, S.; O'Sullivan, R. J.; August, E. M.; Hickey, E. R.; Zhang, Q.; Teodoro, M. L.; Rea, S.; Mechtler, K.; Kowalski, J. A.; Homon, C. A.; Kelly, T. A.; Jenuwein, T. Reversal of H3K9me2 by a small-molecule inhibitor for the G9a histone methyltransferase. *Mol. Cell* **2007**, *25*, 473−481.
(16) Liu, F.; Chen, X.; Allali-Hassani, A.; Quinn, A. M.; Wigle, T. J.; Wasney, G. A.; Dong, A.; Senisterra, G.; Chau, I.; Siarheyeva, A.; Norris, J. L.; Kireev, D. B.; Jadhav, A.; Herold, J. M.; Janzen, W. P.; Arrowsmith, C. H.; Frye, S. V.; Brown, P. J.; Simeonov, A.; Vedadi, M.; Jin, J. Protein lysine methyltransferase G9a inhibitors: design, synthesis, and structure activity relationships of 2,4-diamino-7-aminoalkoxy-quinazolines. *J. Med. Chem.* **2010**, *53*, 5844−5857.
(17) Liu, F.; Barsyte-Lovejoy, D.; Allali-Hassani, A.; He, Y.; Herold, J. M.; Chen, X.; Yates, C. M.; Frye, S. V.; Brown, P. J.; Huang, J.; Vedadi, M.; Arrowsmith, C. H.; Jin, J. Optimization of cellular activity of G9a inhibitors 7-aminoalkoxy-quinazolines. *J. Med. Chem.* **2011**, *54*, 6139−6150.
(18) Vedadi, M.; Barsyte-Lovejoy, D.; Liu, F.; Rival-Gervier, S.; Allali-Hassani, A.; Labrie, V.; Wigle, T. J.; DiMaggio, P. A.; Wasney, G. A.; Siarheyeva, A.; Dong, A.; Tempel, W.; Wang, S.-C.; Chen, X.; Chau, I.; Mangano, T. J.; Huang, X.; Simpson, C. D.; Pattenden, S. G.; Norris, J. L.; Kireev, D. B.; Tripathy, A.; Edwards, A.; Roth, B. L.; Janzen, W. P.; Garcia, B. A.; Petronis, A.; Ellis, J.; Brown, P. J.; Frye, S. V.; Arrowsmith, C. H.; Jin, J. A chemical probe selectively inhibits G9a and GLP methyltransferase activity in cells. *Nat. Chem. Biol.* **2011**, *7*, 566−574.
(19) Liu, F.; Barsyte-Lovejoy, D.; Li, F.; Xiong, Y.; Korboukh, V.; Huang, X.; Allali-Hassani, A.; Janzen, W. P.; Roth, B. L.; Frye, S. V.; Arrowsmith, C. H.; Brown, P. J.; Vedadi, M.; Jin, J. Discovery of an in vivo chemical probe of the lysine methyltransferases G9a and GLP. *J. Med. Chem.* **2013**, *56*, 8931−8942.
(20) Abad-Zapatero, C.; Metz, J. T. Ligand efficiency indices as guideposts for drug discovery. *Drug Discovery Today* **2005**, *10*, 464−469.
(21) Camerino, M. A.; Zhong, N.; Dong, A.; Dickson, B. M.; James, L. I.; Baughman, B. M.; Norris, J. L.; Kireev, D. B.; Janzen, W. P.; Arrowsmith, C. H.; Frye, S. V. The structure-activity relationships of L3MBTL3 inhibitors: A second series of potent compounds which bind the L3MBTL3 dimer. *MedChemComm* **2013**, *4*, 1501−1507.
(22) Tachibana, M.; Ueda, J.; Fukuda, M.; Takeda, N.; Ohta, T.; Iwanari, H.; Sakihama, T.; Kodama, T.; Hamakubo, T.; Shinkai, Y. Histone methyltransferases G9a and GLP form heteromeric complexes and are both crucial for methylation of euchromatin at H3-K9. *Genes Dev.* **2005**, *19*, 815−826.